NPA/Int 64-15
Meyrin, 12th June, 1964.

HIGH ENERGY NEUTRINO INTERACTIONS IN A HEAVY LIQUID BUBBLE CHAMBER

H.H. Bingham[a], H. Burmeister, D.C. Cundy, C. Franzinetti, P.G. Innocenti, A. Lecourtois[b], R. Møllerud[c], G. Myatt, M. Paty, D. Perkins[d]. C.A. Ramm, K. Schultze[e], H. Sletten, K. Soop, R. Stump[f], R.G.P. Voss[g], H. Yoshiki[h].

Abstract

In a sample of 214 neutrino events observed in the CERN heavy liquid bubble chamber, 101 are assigned as examples of the elastic process $\nu + n \rightarrow \mu + p$. The remainder are inelastic events in which one or more pions are created. The energy dependence of the observed cross section for the elastic process is compatible with theoretical predictions. The parameter, M_A, of the axial form factor is found to be ~ 1 Gev. The total cross section for inelastic processes rises rapidly with energy; it is ~ 10 times the elastic cross section at 8 Gev and probably still higher at higher energy. A detailed comparison of inelastic processes with theory is not attempted. Limits are placed for various hypotheses: lepton non-conservation, neutrino flip, neutral lepton currents, neutrino magnetic moment, strange particle production, and the mass of the Tanikawa-Watanabe boson. There is no conclusive evidence for the existence of the intermediate vector boson.

(a) Ford Foundation Fellow
(b) Visitor from Ecole Polytechnique
(c) Visitor from Bergen
(d) Visitor from Bristol
(e) Cern Fellow
(f) Ford Foundation Fellow, visiting scientist from University of Kansas.
(g) Visitor from University of Liverpool
(h) Ford Foundation Fellow, visiting scientist from University of Tokio.

PS/4410

HIGH ENERGY NEUTRINO INTERACTIONS IN A HEAVY LIQUID BUBBLE CHAMBER

1. Introduction

The enhanced neutrino beam installation at CERN enables the study of interactions of either ν_μ or $\bar{\nu}_\mu$ in a heavy liquid bubble chamber. In the present experiments data have been obtained which allow a preliminary comparison of the elastic process with the theoretical predictions[1,2,3] and a determination of the axial form factor involved.

From consideration of lepton conservation, elastic neutrino interactions should be of the form:

$$\nu + n \longrightarrow l^- + p, \tag{1}$$

and inelastic events of the form:

$$\nu + N \longrightarrow l^- + N' + \text{pions}, \tag{2}$$

where l^- is a negative lepton, n a neutron and N and N' are nucleons.

With respect to lepton conservation, and the existence of two neutrinos, our results are in agreement with the work of Danby et al[4]. Thus interactions of ν_μ produce only muons, and ν_e only electrons.

The inelastic processes are not well understood, either experimentally or theoretically; in particular the observed rapid rise of the inelastic cross section with neutrino energy is unexpected.

The intermediate boson W which has been postulated to mediate weak interactions might be expected to be produced incoherently by the process:

$$\nu + p \longrightarrow l^- + W^+ + p, \tag{3}$$

and coherently by:

$$\nu + Z \longrightarrow l^- + W^+ + Z. \tag{4}$$

It has been predicted to decay with a lifetime of $\sim 10^{-16}$ sec:

$$W^+ \longrightarrow l^- + \nu \, , \qquad (5)$$

or

$$W^+ \longrightarrow \text{pionic modes.} \qquad (6)$$

There is no clear evidence in this experiment for possible boson production.

Many aspects of the final analysis cannot be completed without further subsidiary studies, including an attempt to verify experimentally the calculated neutrino spectrum. This report follows the preliminary results(5,6) already given, and is confined to those aspects which are relevant to theoretical predictions, and where interpretations seem unlikely to be affected either by the results of the subsidiary studies or by improved statistics from additional data to be obtained shortly. A more thorough investigation of $\bar{\nu}$ interactions has been deferred until an enlarged bubble chamber becomes available next year.

2. Experimental layout and beam

The principal features of the neutrino experiment include a fast ejection(7) and beam transport system(8) which directs the circulating beam of the proton synchrotron on to an external copper target. Secondary pions and kaons from the target, partially focused by a magnetic horn(9,10), are allowed a free flight of 25 metres in front of a shielding of 23 metres of steel. Neutrinos from the decay of pions and kaons traverse the shielding(11), bubble chamber(12) and spark chamber(13); all other particles are stopped. By changing the sign of the magnetic field in the horn, the neutrino parents can be chosen predominantly positive or negative, thus giving an enhanced ν or $\bar{\nu}$ beam.

The heavy liquid bubble chamber has a total volume of 500 litres in a field of 27 kG, and was filled with freon CF_3Br, which has a density of 1.5 gcm^{-3}, radiation length 11 cm and geometric mean free path 68 cm. The sample of events is from a fiducial volume of 220 litres. Synchronization and sensitivity of the chamber were tested every half hour with a beam of some of the defocused negative particles from the horn.

The 214 neutrino events discussed here were obtained from 3.4×10^{17} ejected protons in 570,000 pulses, with the focusing arranged to give ν_μ. A short run with $\bar{\nu}$ yielded 6 events.

3. Experimental procedure

3.1 Identification of particles

Neutrino events were defined as containing at least one negative track which could be interpreted as a negative muon or electron. Electrons are easily identified in the heavy liquid chamber; negative non-interacting particles were assumed to be muons. A scatter in which the momentum change of the negative track exceeded 100 Mev/c was classed as an interaction. The total length of non-interacting negative track, according to the criteria, is 7875 cm. The total length of light negative track is 8363 cm in which there were 16 interactions assigned as π^-.

Charged kaons of either sign are difficult to identify by ionization, but would have been identifiable by charge exchange. The probability for detection as such is 20 o/o; none was observed. An independent statistical estimate of charged kaons can be made by considering the neutral kaons. The number of K^+ should be comparable to that of K^0, which are easily observable. Two K_1^0 have been assigned; taking into account the K_2^0's not seen, there might be four charged kaons not identified, which would have no significant effect on this analysis.

Positive tracks are due to muons, pions, kaons, or protons. No distinction is attempted here between protons and heavier nuclear fragments, since it is believed such misidentification will also have little effect on this analysis. Protons and pions can usually be identified by ionization and range up to a momentum of 0.7 Gev/c. Below 0.7 Gev/c light positive particles are assumed to be pions if they interacted in the chamber, or if they occurred in an event with a negative lepton. If no negative lepton was present, the non-interacting light positive particles were classified for the present as positive muons from anti-neutrino background. From these criteria the total track length assigned to positive pions is 2390 cm. The mean free path for interaction as a function of energy is consistent with the known energy dependence of the mean free path of π^+. A δ-ray analysis was used to separate statistically protons from pions above 0.7 Gev/c.

Neutral pions have been identified from the kinematical analysis of those events in which both γ's materialised in the chamber. Seven "single γ" events have been found; this number is compatible with the observed number of π^0 and the known detection efficiency of the chamber. Contamination due to inner bremsstrahlung production of single γ's is estimated to be $\sim$2 events.

3.2 Neutron stars

Events with no "lepton candidate" have been interpreted as due to neutrons. Below a visible energy of 250 Mev many have been observed with protons only; between 250 and 275 Mev three have been found, and one at 470 Mev. Fourteen neutron stars associated with pions have been found with energies up to 2.8 Gev.

It is estimated that not more than 4 neutron induced stars have been included among the neutrino events.

4. Classification of events

The simplest event classification is into the processes (1) and (2). However it is quite probable that the produced pions and protons are absorbed or scattered in the nucleus, or even produce additional particles. Table 1 gives a phenomenological classification of events as non-pionic or pionic, which can be considered as an approximation to the elastic and inelastic classification.

There are 21 events which are ambiguous between pionic and non-pionic because there is one unidentifiable fast positive track. These are later referred to as "class C" events. Other ambiguities within the pionic category occur also, and are noted where appropriate.

Most of the elastic events of reaction (1) are included among the 94 non-pionic events of table 1, i.e. those which are associated with a negative track, assumed to be a μ^-, and no possible π. This sample is contaminated by the inelastic events in which the pion is absorbed in the nucleus. A simple kinematic test was used to remove some of this contamination. From the energy and direction of the muon relative to the known neutrino direction, the kinematics of process (1) can be calculated. Since the neutron is in a nucleus its initial momentum is unknown within the limits of Fermi momentum. The calculated energy, E_c , may be compared with the neutrino energy, which is assumed to be E_v , the total visible energy of the event except for the rest masses of the observed nucleons.

It is seen in fig. 1, which shows E_c versus E_v for non-pionic events, that there is a symmetrical distribution about the line $E_c = E_v$. For each elastic event we have calculated the maximum difference which could be produced for a Fermi momentum of 0.27 Gev/c, which is the maximum for a neutron according to the Fermi gas concept of heavy nuclei. In nine cases the observed difference was more than two standard deviations greater than that expected from Fermi momentum alone, and in the sense of $E_v > E_c$ which would be expected for reaction (2) if a pion was absorbed in the nucleus. These nine cases are assumed to be events in which the low energy pion is absorbed in the nucleus and are therefore assigned as pionic. An estimate of the number of pions reabsorbed in nuclear matter, based on experimental data on pion absorption by nuclei and the observed pion spectrum in the neutrino events, suggests that 13 inelastic events in which the π was absorbed are still present in the assigned "elastic" events.

The same kinematical test was made for the 97 pionic events and is shown in fig. 2, which has a markedly different distribution from fig. 1; there is an excess of events, all in the sense $E_v > E_c$. It is concluded that most pionic events are due to a primary inelastic process. Less than 2.5 o/o of elastic events should appear pionic due to a pion produced in the same nucleus by the recoil proton; this contamination has been neglected.

Two of the 21 "class C" events were incompatible with the elastic hypothesis, and for the remaining 19 a δ-ray count suggests most are protons. An estimate gives 3 pions to 16 protons, which would justify an assignment as predominantly elastic events.

A mass M^* required by energy and momentum conservation in the process $\nu + N \rightarrow \mu^- + M^*$ has been calculated from the muon momentum and E_V with the assumption that the target nucleon is at rest. In addition to measurement errors, there are uncertainties in this calculation due to Fermi motion of the neutron and the assumption that the neutrino energy is E_V, which is in fact only a lower limit since both pions and protons may lose energy in the nucleus in which the interaction occurs. Fig. 3 shows M^* calculated for the class C events with the assumption that the uncertain track is due to a proton; the grouping of M^* around the proton mass is consistent with this assignment of the uncertain track. However, if the uncertain track is assumed to be a pion, the same calculation leads to a M^* which is consistent with that of identified pionic events, and thus no clear assignment of the "C" events is possible. They are shown in the distributions with each interpretation.

5. Analysis of elastic events

5.1. Energy dependence of the cross section

Fig. 4a shows the experimental energy and the event rate of the 84 elastic events. The shading shows the 19 class C events of the previous section, the curve represents the absolute expected energy distribution calculated from the theoretical cross section and the calculated neutrino spectrum. To show various implications of fig. 4, the same data are also shown in the two succeeding figures.

From the calculated ν spectrum[10] the cross section can be deduced, as is shown in fig. 4b together with the theoretical cross section.[1,2,3] The calculated neutrino spectrum is shown in fig. 5, as well as the spectrum deduced from the event rate and the theoretically predicted dependence of cross section on neutrino energy.

At this stage the uncertainties in the knowledge of the neutrino spectrum and possible experimental biases are such that any agreement between the experimental results and theoretical predictions cannot be considered highly significant. Further studies now in progress on pion production in the copper target of the horn and pion absorption in the nuclei, as well as improved statistics, will allow a more precise comparison between theory and experiment in the near future.

5.2 Four momentum transfer distribution

In order to investigate the form factors pertinent to the elastic interactions[14] the 4-momentum transfer in the ν-μ system has been calculated. Two methods may be used for calculating q^2: either from the observed momentum of the muon and the assumption that E_v is the neutrino energy, or from the muon momentum alone, using the kinematics of (1) and assuming that the target neutron is initially at rest. The distributions obtained are essentially the same; the results of the first method have been used for comparison with the theoretical predictions in fig. 6. The matrix element describing elastic interactions is expected to be of the form:

$$M = (G/\sqrt{2})\ \bar{u}_p \left\{ F_1\gamma_\lambda - (\Delta\mu/2M_p)\ F_2\ \sigma_{\lambda\mu}\ q_\mu + \lambda F_A\gamma_\lambda\gamma_5 \right\} u_n\ \bar{u}_e\gamma_\lambda\ (1+\gamma_5)u_\nu$$

the induced pseudoscalar term having been neglected. The curves of fig. 6 have been calculated taking the form factors [15] to be

$$F_1 = F_2 = F_{EM} = (\ 1 + q^2/M_{EM}^2\ )^{-2} \qquad (M_{EM} = 0.84 \text{ Gev})$$

and the axial form factor,

$$F_A = (\ 1 + q^2/M_A^2\ )^{-2}$$

and $\lambda = 1.25$. If the interaction is considered to be mediated by an intermediate vector boson of finite mass M_W, the form factors must be multiplied by

$$(\ 1 + q^2/M_W^2\ )^{-1}$$

The theoretical distribution based on the calculated neutrino spectrum is corrected for the effects of Fermi momentum, exclusion principle and experimental resolution.

Various values of the parameter M_A and of the mass M_W have been considered, and the statistics of the fit of the experimental results examined for events with $q^2 < 1.2\ (\text{Gev/c})^2$. Equally good fits can be obtained with any value of M_W in the range 1.3 Gev to infinity, provided M_A is varied accordingly. If $M_W = \infty$, and all class C events are included, M_A is found to be less than

1.35 Gev with a confidence limit of 68 o/o, the best fit being obtained for $M_A = 1.0$ Gev. For comparison, the expected distribution for $M_A = 1.8$ Gev has also been plotted.

If none of the ambiguous events is included, M_A is found to be smaller than 1.0 Gev, with 68 o/o confidence limit, the most probable value being $M_A = 0.85$ Gev.

On the basis of the q^2 distribution alone, $M_A = 0$ cannot be excluded. However, a lower limit for M_A can be deduced from the difference between the cross sections for elastic interactions of neutrinos and anti-neutrinos. Such a difference is proportional to

$$q^2 \lambda \left(F_1 + (\triangle_\mu / 2M_p) F_2 \right) F_A,$$

from which, if F_1 and F_2 are known, F_A can be deduced. Of the six events observed in the $\bar{\nu}$ exposure not more than 3 could be attributed to elastic events, whereas for a ν exposure of equal flux, 10 events would have been expected. This sets a lower limit for $M_A = 0.4$ Gev with 68 o/o confidence. This method of estimating M_A is very sensitive to the ν and $\bar{\nu}$ spectra, neither of which are well known. It would lead to the conclusion, assuming $M_W = \infty$ and C.V.C. theory, that M_A is within the range 0.4 to 1.35 Gev with 68 o/o confidence, the most probable value being about 1.0 Gev. $M_A = \infty$ is excluded. Similar conclusions have been reached by the spark chamber group[13] from a study of the angular distribution of muons.

5.3 Distribution of momentum unbalance

The momentum unbalance of the one proton elastic event is

$$P^2 = (p_\mu + p_p)_y^2 + (p_\mu + p_p)_z^2 + (E_\nu - (p_\mu + p_p)_x)^2$$

as shown in fig. 7, where the quantity $\triangle N / \triangle P$ is plotted as a function of P, N being the number of events.

The statistical uncertainties are large, but it can be seen that for $P < 0.3$ Gev/c the rise in the distribution is similar to P^2, as would be expected for the Fermi momentum of the target neutron in a heavy nucleus.

However, about half of the events have $P > 0.4$ Gev/c, which may be due to scattering of the recoil proton inside the nucleus, the residual momentum escaping detection when absorbed by heavy fragments too short to be detected, or by neutrons which do not interact in the chamber. Events with higher multiplicities have no significance for determining the Fermi distribution.

6. Analysis of the inelastic events

6.1. Single pion events

The assignment to single pion events totals 60. They comprise 49 events with one identified pion ; 2 ambiguous events, which were not kinematically consistent with "elastic" when the ambiguous track was assumed to be a proton; and 9 non-pionic events similarly incompatible with "elastic", and which have been taken as cases in which a pion was created and subsequently reabsorbed. There are also 12 events which have one identified pion and one ambiguous track (1 π, 1 c). Table 2 gives other details.

No conclusive interpretation of these events has been found. Two processes which would create pions in neutrino events have been predicted: via the production of the 3/2, 3/2 N^* isobar(16), and in peripheral interactions with single pion exchange.(16,17) For the present we see no clear way to identify the two processes because of the nuclear interactions of both protons and pions and the N^* itself.

The experimental cross section as a function of the visible energy is shown in fig. 8; the total rate is comparable with the elastic rate. The energy dependence of M^* and q^2 are shown in Figs. 9 and 10.

The average value of M^* rises slowly with E_v. The production of pions via the 3/2, 3/2 N^* isobar is expected to take place to some extent, and in such a plot it would show as a concentration around a horizontal line at the N^* mass. It is impossible to estimate the production rate from the statistics of fig. 9. It would be expected that the charge distribution of single pion events associated with the isobar would be $(p,\pi^+) : (p,\pi^c) : (n,\pi^+) = 9 : 2 : 1$ whereas for events with not more than one proton it is in fact 19 : 6 : 9. The distortion of the original charge distribution due to secondary interactions of pions while traversing the nucleus is unknown; subsidiary studies to assess such effects are being made.

6.2 Energy dependence of the inelastic cross section

The E_ν distribution of all inelastic events and the inelastic cross section σ_{in}, as computed from the observed rates using the calculated ν spectrum, are shown in fig. 11. There is a rapid rise of σ_{in} with energy, but beyond 4 Gev the experimental errors are large. However, one neutrino event has been observed with $E_\nu \sim 12$ Gev, and one with ~ 14 Gev. The ν flux between 10 to 15 Gev is estimated to be some two orders of magnitude less than that between 5 to 10 Gev. Thus the presence of these events is significant, and it is inferred that σ_{in} is still rising with energy up to 14 Gev.

7. Other results and conclusions

7.1 Lepton conservation

Most of the events observed in this experiment demonstrate lepton conservation of the $\nu_\mu - \mu$ system; the events are of the type :

$$\nu_\mu + N \longrightarrow \mu^- + \text{non-leptonic particles} \tag{7}$$

Two types of lepton non-conservation which could be observed, if present, are :

$$\nu_\mu + N \longrightarrow \text{non-leptonic particles} \tag{8}$$

$$\nu_\mu + N \longrightarrow \mu^+ + \text{non-leptonic particles} \tag{9}$$

An event of type (8) is indistinguishable from a neutron induced event and since there is a significant low energy neutron background, an upper limit on the process can be set only at high energy. Two events without leptons and with $E_\nu > 1$ Gev have been observed; both may be attributed to neutrons. However, if they are assumed to be due to (8), one can set an upper limit on this type of lepton non-conservation of ~ 4 o/o of the total event rate for neutrino interactions above 1 Gev.

In connection with (9), there are 16 events with a possible μ^+, and no μ^-, which is consistent with the calculated $\bar{\nu}_\mu$ background, and they have been thus assigned. Assuming no $\bar{\nu}_\mu$ background gives a rate of ~ 9 o/o as an upper limit for (9).

7.2 The existence of two neutrinos

The present observations confirm the existence[4] of two types of neutrinos, ν_e and ν_μ. The neutrino flux through the bubble chamber is predominatly ν_μ with a small background of ν_e from the K^+_{e3} decay, so that most of the events should be associated with muons. Among the 85 unambiguous elastic events there is one in which the lepton is e^-, all others have μ^-. This agrees with the spark chamber result[13] of (1.1 ± 0.4)o/o for the ratio of elastic e to μ production. In the inelastic events, three e^- and 106 μ^- were observed. About three e^- events are expected from K^+_{e3} neutrinos; the uncertainty in the estimate is such that the observed rate is certainly consistent with this estimate.

7.3 Neutrino flip

It has been suggested[18] that in kaon decay the usual (ν_μ, μ^-), (ν_e, e^-) pairings are reversed, e.g.

$$K^+_\mu \rightarrow \mu^+ + \nu_e \qquad (10)$$

Following this hypothesis, 5 o/o of all neutrinos would be ν_e. Only four events in which the lepton is an e^- have been observed, at least eleven are expected from the neutrino flip hypothesis. Thus the neutrino flip hypothesis is not necessary to account for the observations.

7.4 Strange particles

In 3 events strange particles have been identified: a single Λ, a single K^o, and one event with both Λ and K^o. Both of the Λ's decayed in the charged mode; one of the K^o gave $\pi^+ + \pi^-$, and the other two π^o's. The event with the single K^o contained in addition an isolated electron pair, which could have come from the π^o of the neutral decay of a Λ. Each of the events had $E_\nu > 4$ Gev.

Single production of strange particles is of importance in connection with the $\frac{\Delta Q}{\Delta S} = 1$ rule, which imposes a number of restrictions on the possible reactions. The three events are probably not pertinent to this rule, because it is expected* that events with strange particle production will have an energy distribution similar to the elastic events, which do not extend beyond 4 Gev. It seems reasonable to assume that they are examples of associated production connected with strangeness conserving vertices.

7.5 Neutral lepton currents

Reactions such as

$$\nu + p \longrightarrow \nu + p \qquad (11)$$

$$\nu + N \longrightarrow \nu + N + \text{pions} \qquad (12)$$

may indicate the existence of neutral lepton currents, but experimentally they are indistinguishable from lepton non-conserving or from neutron-induced events. Due to the neutron background we determine a limit on such processes only at high q^2, in comparison with the corresponding charged-current induced elastic or inelastic process.

Among the events with a visible non-leptonic energy in excess of 275Mev, which corresponds to $q^2 \sim 500$ Mev/c^2 for process (1) with zero Fermi momentum, one was observed with nucleons and no lepton, which is thus a candidate for (11). Among the elastic and ambiguous neutrino events there are 32 which are associated with nucleons of a total kinetic energy exceeding 275 Mev. Thus the cross section for (11) is estimated to be less than 3 o/o of that of the elastic process producing a charged lepton with $q^2 \sim 500$ (Mev/c)^2.

Fourteen events associated with nucleons and pions only were found, with a visible energy above the limit of 275 Mev. If all were attributed to (12) the upper limit for the process would be 6 o/o of the total cross section for ν - interactions.

---

* We thank Prof. M. Block for enlightening discussions on this point.

7.6 Upper limit to the magnetic moment of ν_μ

Even in the absence of neutral lepton currents, the processes

$$\nu_\mu + e \longrightarrow \nu_\mu + e \qquad (13)$$

$$\nu_\mu + p \longrightarrow \nu_\mu + p \qquad (14)$$

could take place via an electromagnetic interaction,[19] if the neutrino possessed a magnetic moment. About 7 o/o of the photographs were scanned for isolated electron production; no single electron was found with an energy of more than 25 Mev. This sets an upper limit for the magnetic moment of ν_μ of $\sim 10^{-6}$ Bohr magnetons. From the absence of single proton events with an energy above 275 Mev, we can give an upper limit of $\sim 10^{-7}$ Bohr magnetons.

7.7 Lepton pairs - The intermediate boson and other postulated particles

Lepton pairs in neutrino interactions are of interest in connection with the production of the vector boson W, which has been postulated[20,21] to be produced according to (3). The branching ratios and the nature of the strongly interacting particle decay modes are unknown. Due to the short lifetime of the boson the decay products would appear to come from the primary interaction.

Both the leptonic and non-leptonic decay modes of the W have been sought in this experiment. The leptonic decays would be expected to appear as events with two leptons, a μ^- by definition, and either μ^+ or e^+, with perhaps also one or more protons. Since the bubble chamber gives no basis for distinguishing μ^+ from π^+ for non-interacting tracks, nothing can be said concerning (μ^+, μ^-) events except that there are some which could be consistent with such interpretation. A production rate of 0.5 to 1 o/o of all neutrino events, tentatively suggested by the spark chamber group[13] would be impossible for us to detect. However, e^+ are easily identifiable by bremsstrahlung. Of the 213 neutrino events observed, one was found with a non-interacting negative meson track and a shower. Parameters of this candidate for interpretation as a (μ^-, e^+) pair are shown in table 3.

Table 3 - Parameters of the (μ^-, e^+) candidate

E_ν (Gev)	E_{μ^-} (Gev)	E_{e^+} (Gev)	Cos θ_{e^+}	Cos θ_μ	Momentum un-balance (Gev/c)
1.79	0.48	1.22 ± 0.3	0.956	.836	P = 0.28

It is impossible to be certain of the identification of either of the two lepton candidates. The negative meson track of 40 cm could be either a μ^- or a π^-. The nature of the particle initiating the shower is also doubtful: it could be a positron or a narrow Dalitz pair.

The significant attribution of a single event with a lepton pair to the boson is impossible because an unseen neutrino would be involved in the boson decay. Also lepton pairs may be produced through a four-fermion point interaction and subsequent scattering of the charged lepton in the Coulomb field of the nucleus. However the cross section for such a process is estimated[22] to be so much smaller than the elastic cross section that it should not give any significant contribution to lepton pair production.

Multipion events have been analysed for evidence of the pionic decay of the boson. the invariant mass of all pions in each event for which the charge of the pion combination is + 1 is shown in fig. 12. Events outside the fiducial volume are included, and events may occur more than once according to various possible interpretations. From this diagram, with the presently available statistics, it would be impossible to identify a boson.

Another type of boson has also been considered[23,24] as the mediator of weak interactions. Such bosons (W') would produce resonances of the type:

$$e^- + p \longrightarrow W' \longrightarrow e^- + p \qquad (15)$$

$$\nu_\mu + n \longrightarrow W'_\mu \longrightarrow \mu^- + p \qquad (16)$$

A lower limit on the mass of a possible boson W' of (15) has been set by Allaby et al[25]. The limit on the mass of W' and W'_μ can be raised from the results of this present experiment.

According to the predictions, the resonance of (16) would have a cross section of $\sim 10^{-26}$ cm^2 and a width of $\sim$100 ev. Fermi momentum of the target nucleon would give an apparent cross section of $\sim 10^{-32}$ cm^2, and an apparent width of $\sim$0.5 Gev, to be compared with an elastic ν cross section of $\sim 10^{-38}$ cm^2. At 10 Gev, the neutrino flux is estimated to be $\sim 10^{-4}$ of that at 1 Gev. Thus from the elastic event rate at 1 Gev, if the predicted phenomena existed at $\sim$10 Gev some 10^3 events/Gev would be expected. If the two events which were observed with E_ν >10 Gev were attributed to W'_μ the predicted cross section would still be too large by $\sim 10^3$. Therefore we conclude that the threshold for the predicted boson must be above 10 Gev, and that its mass is greater than 4.2 Gev.

8. Acknowledgements

The neutrino experiment is especially indebted to Professors V.W. Weisskopf and G. Bernadini for their sustained enthusiasm, support and encouragement.

We have deeply appreciated the collaboration of J.S. Bell, M. Block, J. Løveseth, M. Nikolic and M. Veltman.

The observation of neutrino events in the heavy liquid bubble chamber was the culmination of technological development by many groups. It is with pleasure and gratitude that we acknowledge the construction and operation of the enhanced neutrino beam by M. Giesch, B. Kuiper, B. Langeseth, S. van der Meer, S. Pichler, G. Plass, G. Pluym, K. Vahlbruch, H. Wachsmuth and their colleagues; the operation and development of the heavy liquid bubble chamber,

and the continued efforts to obtain the highest possible beam by the members of the Proton Synchrotron Division.

Finally, our warmest thanks to "the scanning girls" for their unstinted efforts and care with the data handling.

References

1. T.D. Lee and C.N. Yang, Phys. Rev. Letters 4, 307, 1960
2. N. Cabibbo, R. Gatto, N. Cim. 15, 304, 1960
3. Y. Yamagu chi, Prog. Theor. Phys. 23, 117, 1960
4. G. Danby et al, Phys. Rev. Letters 9, 36, 1962
5. R.G.P. Voss, Brookhaven* 114, 1963 and CERN 61-2
6. Perkins et al, Sienna** 555, 1963
7. B. Kuiper et al, Dubna Int. Conference on High Energy Accel. 1963 to be published.
8. G. Plass et al, Sienna** 523, 1963
9. S. van der Meer, Nucl. Inst. 20, 58, 1963
10. S. van der Meer , Sienna** 536, 1963
11. C.A. Ramm, Brookhaven* 91, 1963
12. C.A. Ramm and L. Resegotti, proceedings Int. Conference on Instr. for High Energy Phys., Interscience Publishers, New York, 127, 1960
13. H. Faissner, Brookhaven* 137, 1963
    G. Bernardini et al, Sienna** 571, 1963
14. J. Løveseth, Private communications
15. R. Hofstadter, Rev. Mod. Phys. 28, 214, 1956 and 30, 482, 1958
16. J.S. Bell, S.M. Berman, N. Cim. 25, 404, 1962
17. N. Cabibbo, G. da Prato, N. Cim. 25, 611, 1962
18. G. Feinberg, F. Gürsey, A. Pais, Phys. Rev. Letters 7, 208, 1961
19. H. Bethe, Proc. Cambridge Phil. Soc. 31, 108, 1935
    C.L. Cowan, F. Reines, Phys. Rev. 107, 528, 1957
20. J. Schwinger, Ann. Phys. 2, 407, 1957
21. T.D. Lee, C.N. Yang, Phys. Rev. 119, 1410, 1960
22. W. Czyz, G.C. Sheppey, J.D. Walecka, to be published.
23. Y. Tanikawa, S. Watanabe, Phys. Rev. 113, 1344, 1959
24. T. Kinoshita, Phys. Rev. Letters, 4, 378, 1960
25. J.V. Allaby et al, Phys. Rev. 133, B 1514, 1964

---

* International Conference in fundamental aspects of Weak Interactions Brookhaven, Sept. 1963.

** International Conference on elementary particles, Sienna October, 1963.

Figure Captions

Fig. 1. A plot of E_c versus E_ν for non-pionic events.

2. A plot of E_c versus E_ν for pionic events.

3. M^* versus E_ν for elastic and class C events.

4. Energy Spectrum and Cross-section for elastic events.

5. Experimental estimation of ν spectrum, compared to the calculated spectrum.

6. Four-momentum transfer distribution for elastic events.

7. Distribution of momentum unbalance for 1 proton elastic events.

8. Energy spectrum and cross-section for 1 π events.

9. M^* versus E_ν for all inelastic events. (The multipion events include 1 π, 1 C)

10. q^2 versus E_ν for all inelastic events. (" " " " ")

11. Energy spectrum and cross-section for all inelastic events.

12. Invariant Mass distribution of all pions in those events where the total charge of the pions is + 1.

13. An example of an inelastic event; probably of the form

$$\nu + p \longrightarrow \mu^- + N + \pi^+ + \pi^+ + \pi^0$$

Table 1: Observed rates of ν - events

Phenomenological Classification		Assigned Interpretation	
Type	Number	Elastic	Inelastic
non pion μ events	93	84	9
non pion e events	1	1	0
pion μ events	95^{*}	0	95
pionic e events	3^{**}	0	3
class C μ events	21	16	5
class C e events	0	0	0
possible μ^{-} e^{+} pair	1	0	1
Total	214	101	113

* Includes 1 event with K^{o} and 1 event with $\Lambda + K^{o}$

** Includes 1 event with Λ .

Table 2: Pion multiplicity of inelastic events.

(Events with unidentified tracks included only once, with assignment of highest multiplicity)

Visible Pion Multiplicity	Type	Visible Energy (Gev) <1	1 - 2	2 - 3	3 - 4	4 - 8	8 - 14	Total
0	non pionic*	3	2	1	2	1	-	9
1	1 π assigned	21	19	2	3	4	-	49
	1 π class C*	-	1	1	-	-	-	2
	1 π class C**	1	9	7	-	2	-	19
2	2 π assigned	2	3	2	1	-	-	8
	1 π, 1 track unidentified	-	6	4	0	2	-	12
	2 tracks unidentified	-	1	-	1	-	-	2
3	3 π assigned	-	2	1	1	5	-	18
	Assigned with $\Lambda + K^0$	-	-	-	-	1	-	
	2 π, 1 track unidentified	-	1	-	2	2	-	
	1 π, 2 tracks unidentified	-	-	2	1	-	-	
4	4 π assigned with K^0	-	-	-	-	1	-	
	3 π, 1 track unidentified	-	-	-	1	1	-	
	2 π, Λ, 2 tracks unidentified	-	-	-	-	1	-	
5	5 π assigned	-	-	-	-	1	-	9
	4 π, 1 track unidentified	-	-	-	-	1	-	
6	6 π assigned	-	-	-	-	1	-	
	5 π, 1 track unidentified	-	-	-	-	-	1	
	4 π, 2 tracks unidentified	-	-	-	-	-	1	
	Totals	27	44	19	12	23	2	128

* Assigned as inelastic from kinematical analysis

** These are class C events which cannot be assigned from kinematical analysis. From δ-ray analysis it is estimated among the 19 events there are only 3 pionic.

Table 3: See Page 14.

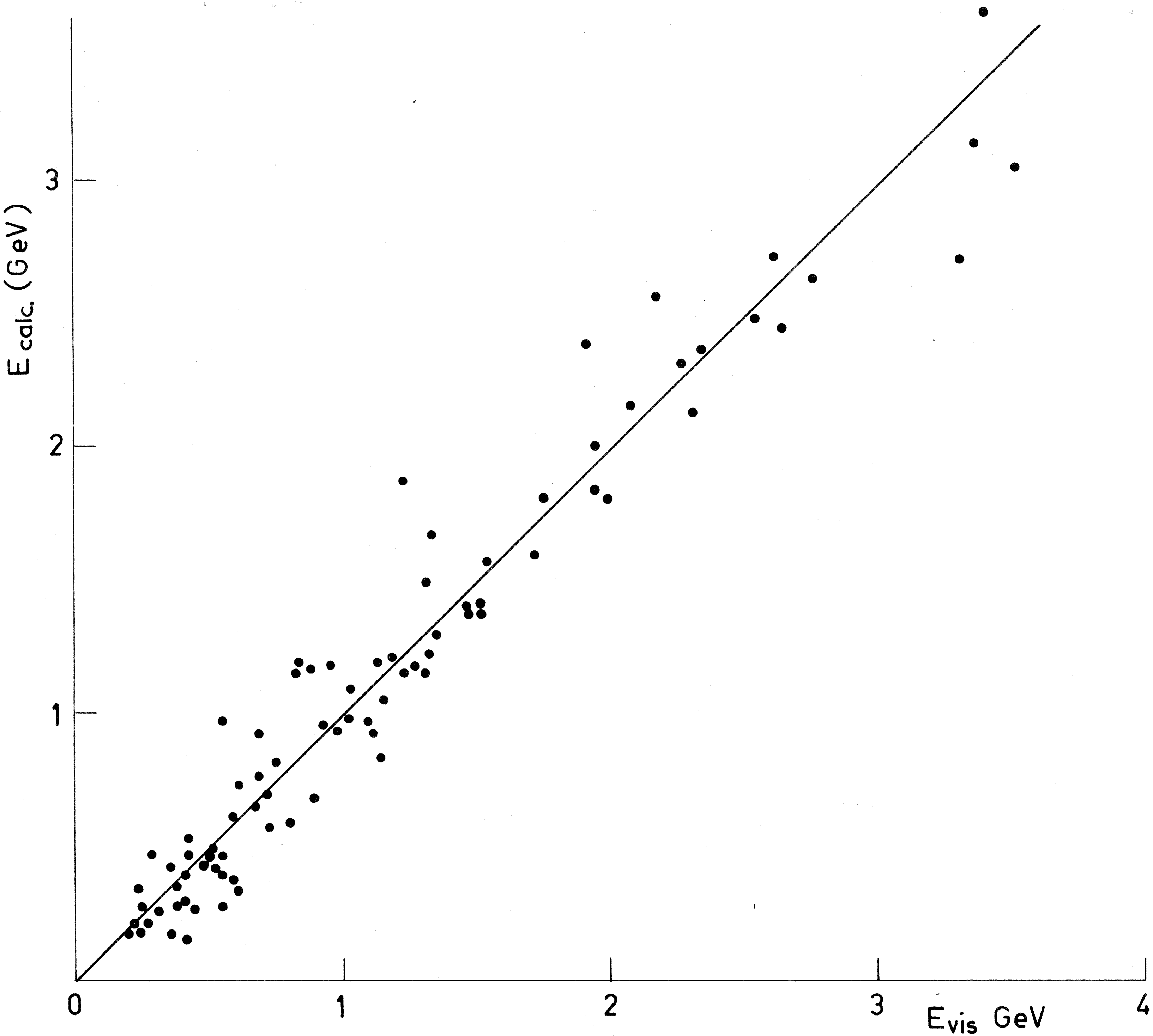

E calc. (GeV)
3
2
1
0
1
2
3
4
Evis GeV

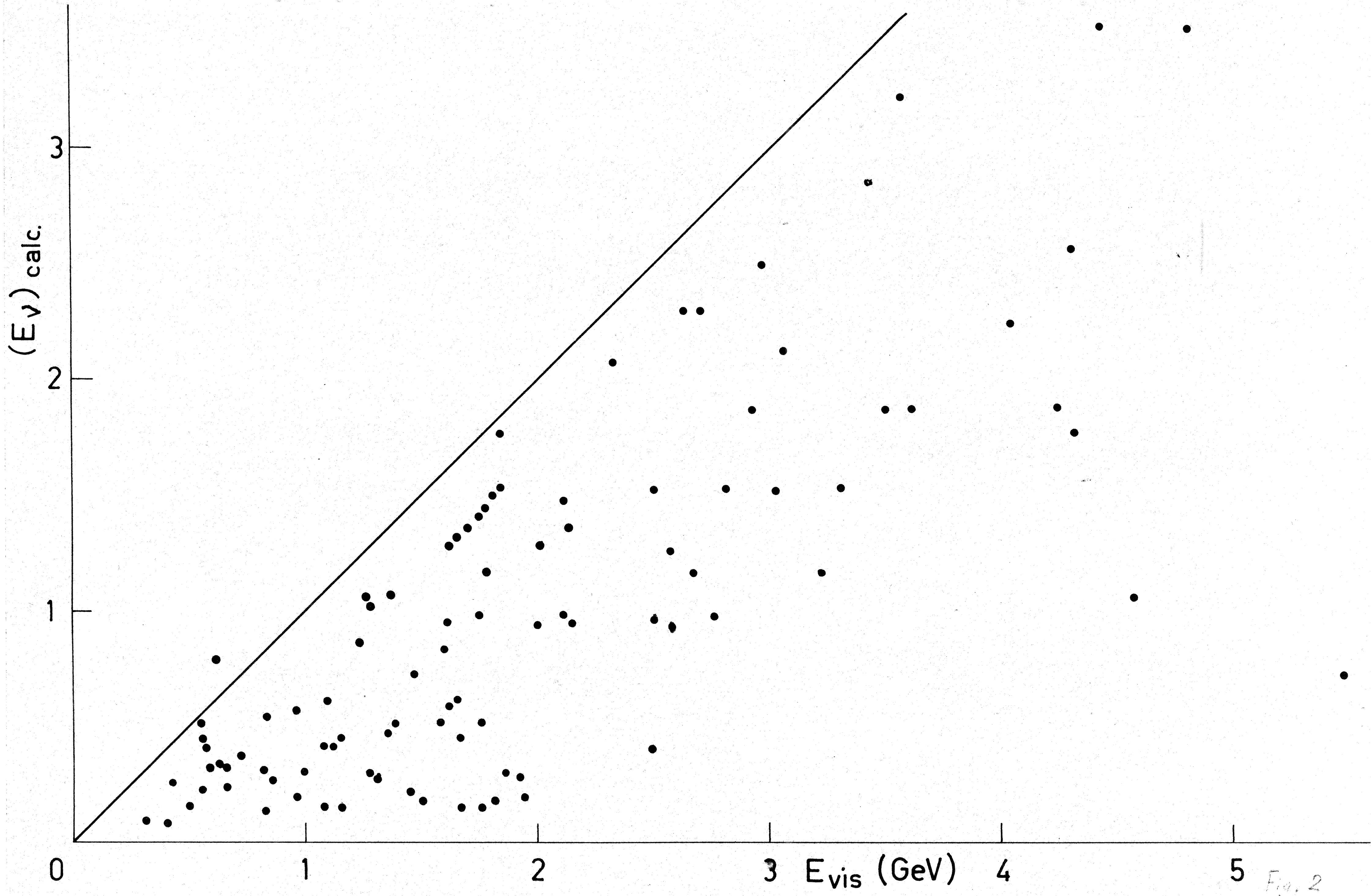

Fig. 2

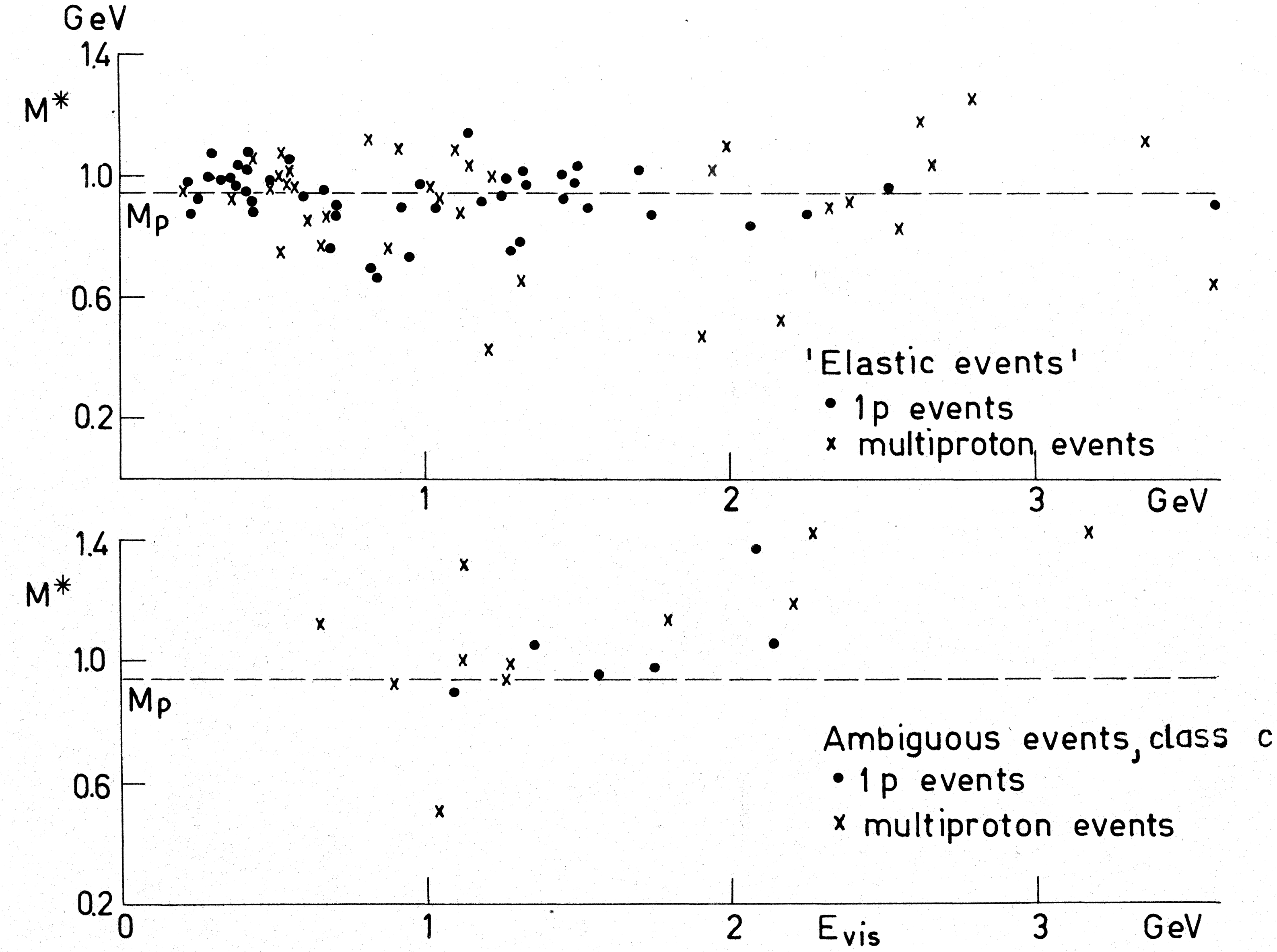
GeV
1.4
M*
1.0
Mp
0.6
0.2
'Elastic events'
• 1p events
x multiproton events
1
2
3
GeV
1.4
M*
1.0
Mp
0.6
0.2
Ambiguous events, class c
• 1p events
x multiproton events
0
1
2
Evis
3
GeV

Fig. 3

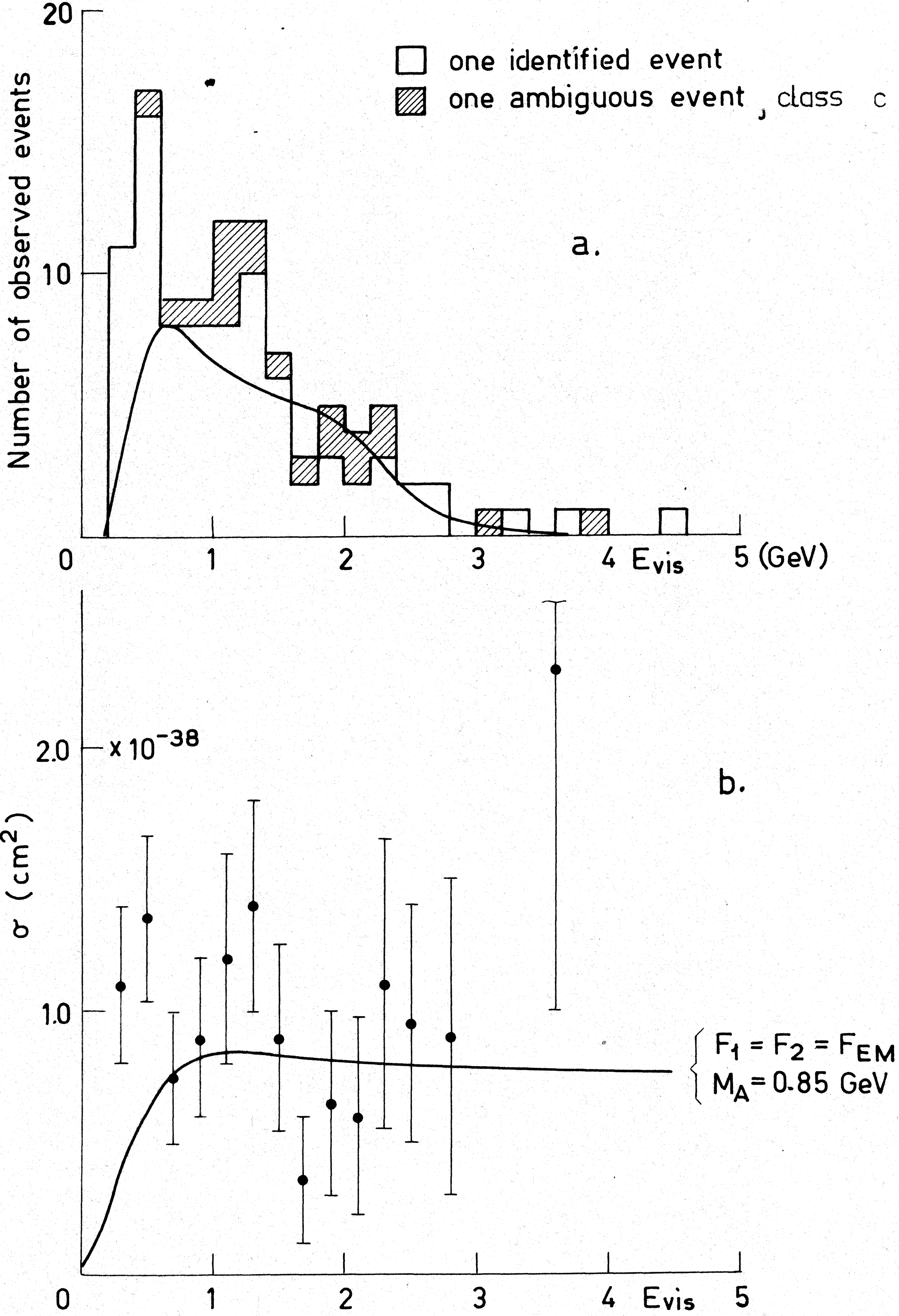
one identified event
one ambiguous event , class c
Number of observed events
a.
20
10
0
1
2
3
4
5 (GeV)
E_{vis}
σ (cm^2)
$\times 10^{-38}$
2.0
1.0
b.
$F_1 = F_2 = F_{EM}$
$M_A = 0.85$ GeV
Evis

Fig 4

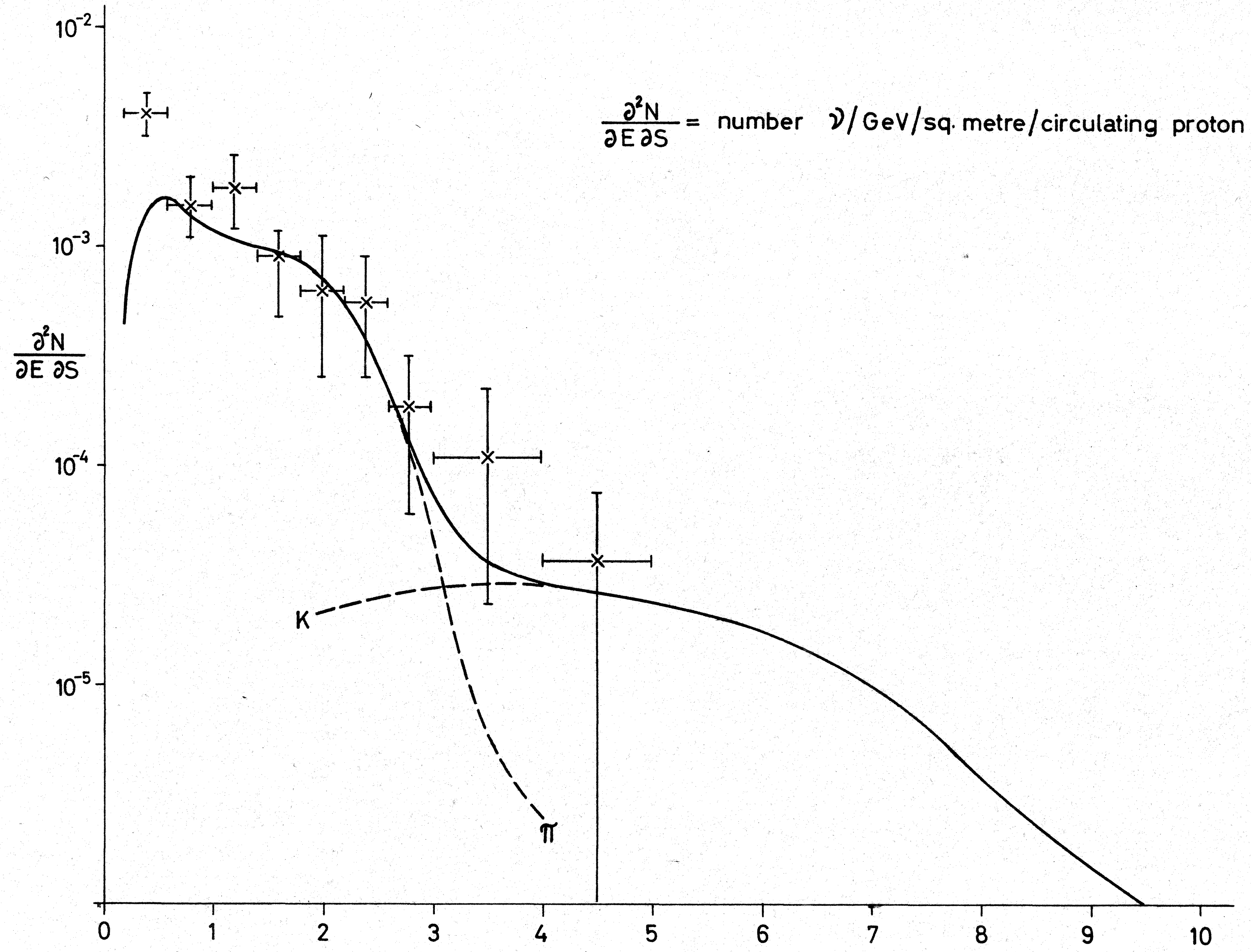
$\frac{\partial^2 N}{\partial E \, \partial S}$ = number ν/GeV/sq. metre/circulating proton
10^{-2}
10^{-3}
10^{-4}
10^{-5}
$\frac{\partial^2 N}{\partial E \, \partial S}$
K
π
0
1
2
3
4
5
6
7
8
9
10
ν energy GeV

Fig. 5

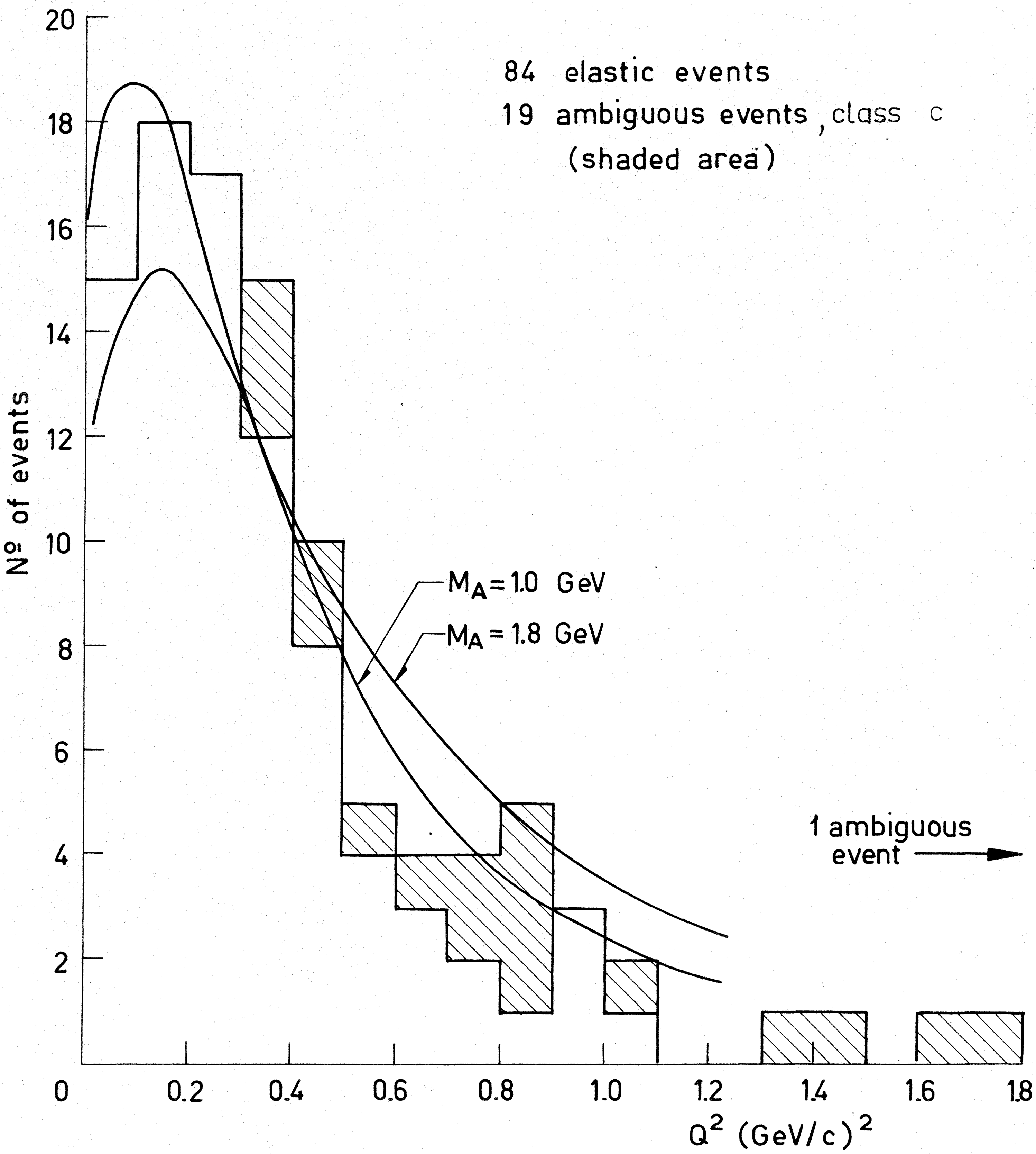
84 elastic events
19 ambiguous events, class c
(shaded area)
$M_A = 1.0$ GeV
$M_A = 1.8$ GeV
1 ambiguous event
Nº of events
20
18
16
14
12
10
8
6
4
2
0
0.2
0.4
0.6
0.8
1.0
1.2
1.4
1.6
1.8
Q^2 (GeV/c)^2

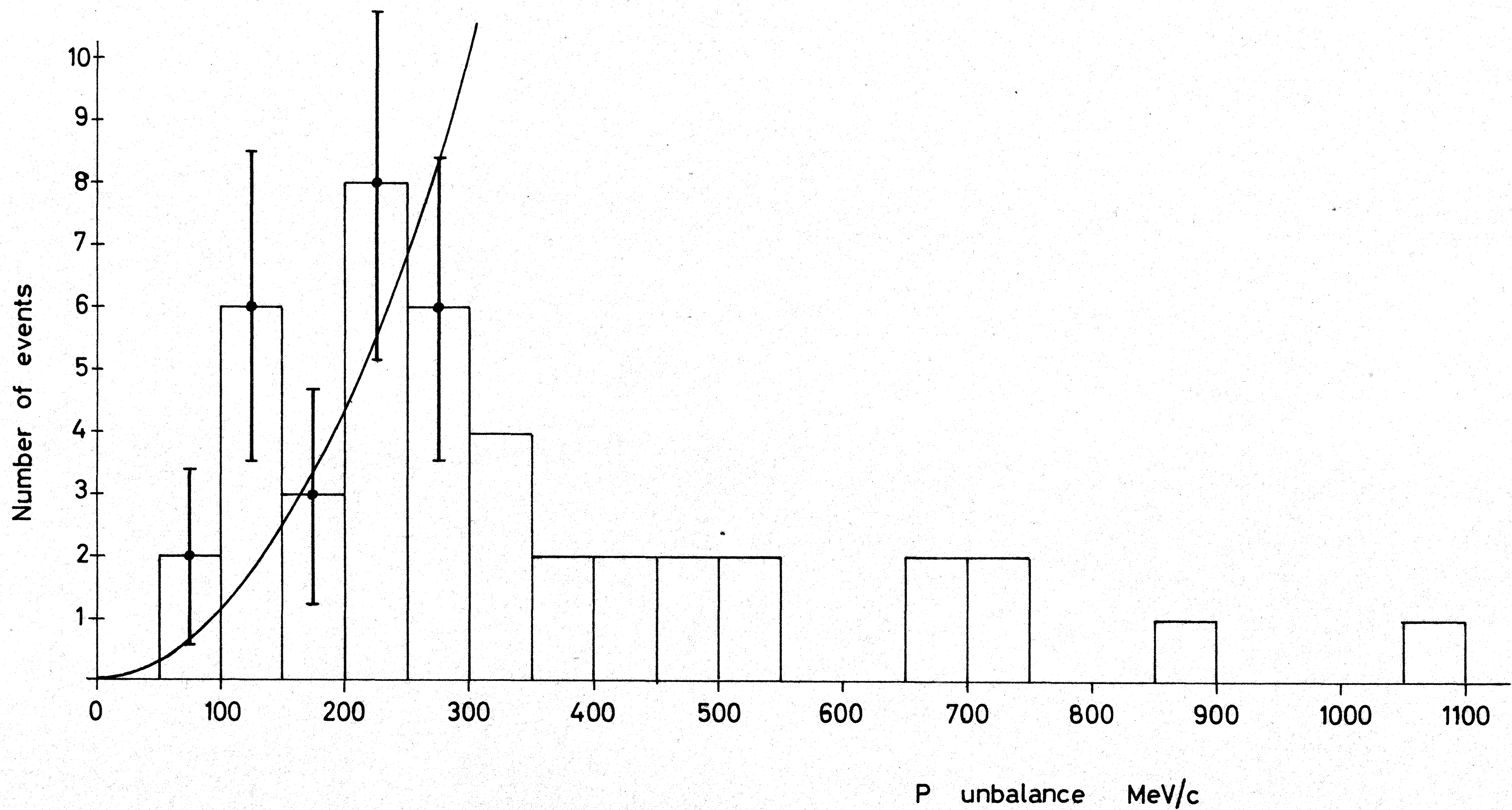
Number of events
10
9
8
7
6
5
4
3
2
1
0
100
200
300
400
500
600
700
800
900
1000
1100
P unbalance MeV/c

Fig. 7

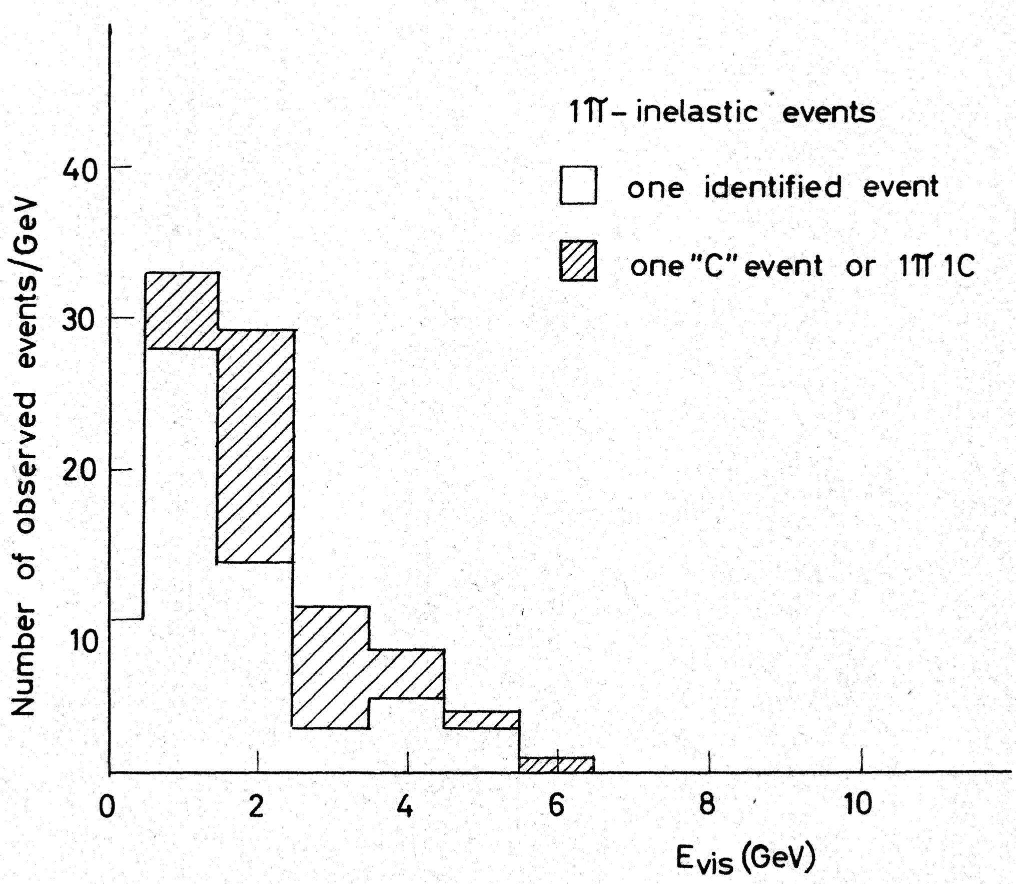
1π - inelastic events
one identified event
one "C" event or 1π 1C
Number of observed events/GeV
40
30
20
10
0
2
4
6
8
10
E_{vis} (GeV)

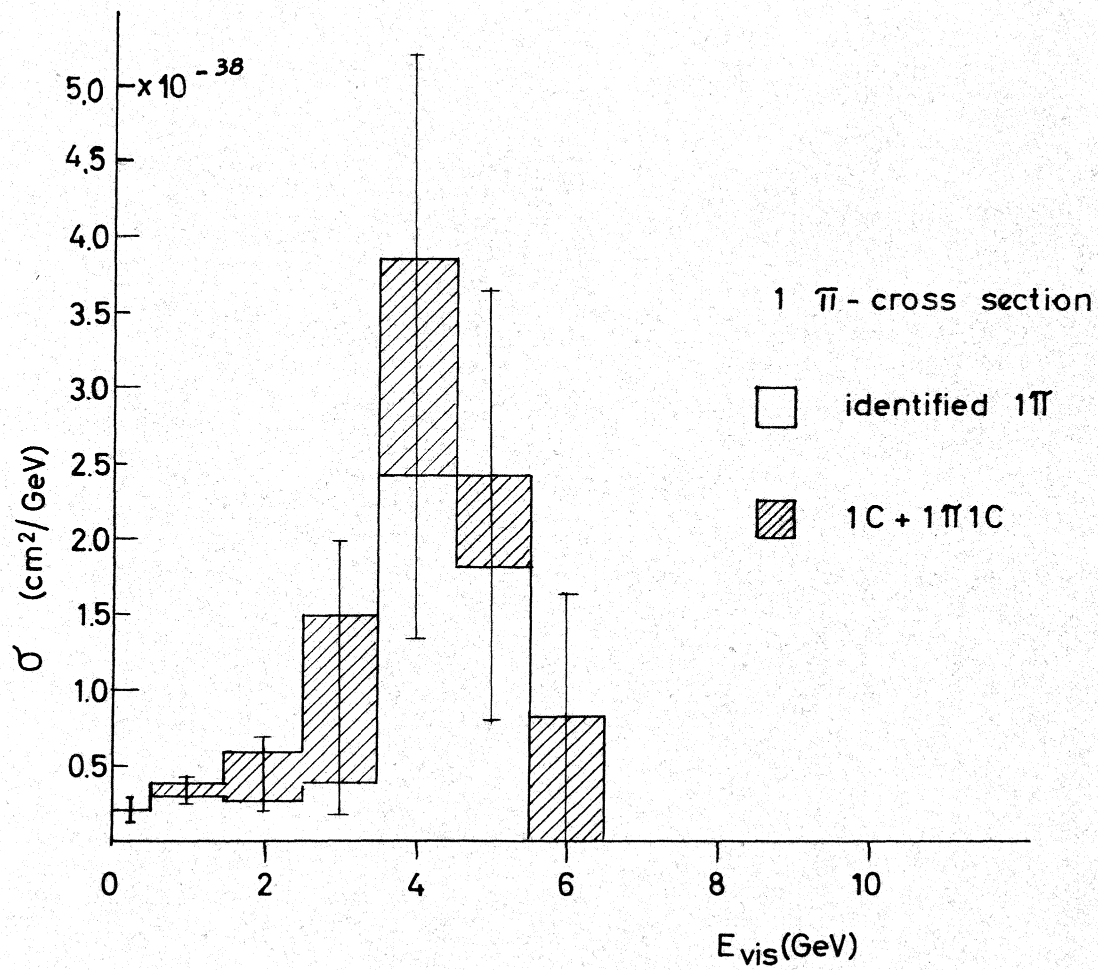
$\times 10^{-38}$
5.0
4.5
4.0
3.5
3.0
2.5
2.0
1.5
1.0
0.5
σ (cm²/GeV)
1 π - cross section
identified 1π
1C + 1π 1C
0
2
4
6
8
10
E_{vis} (GeV)

Fig. 8

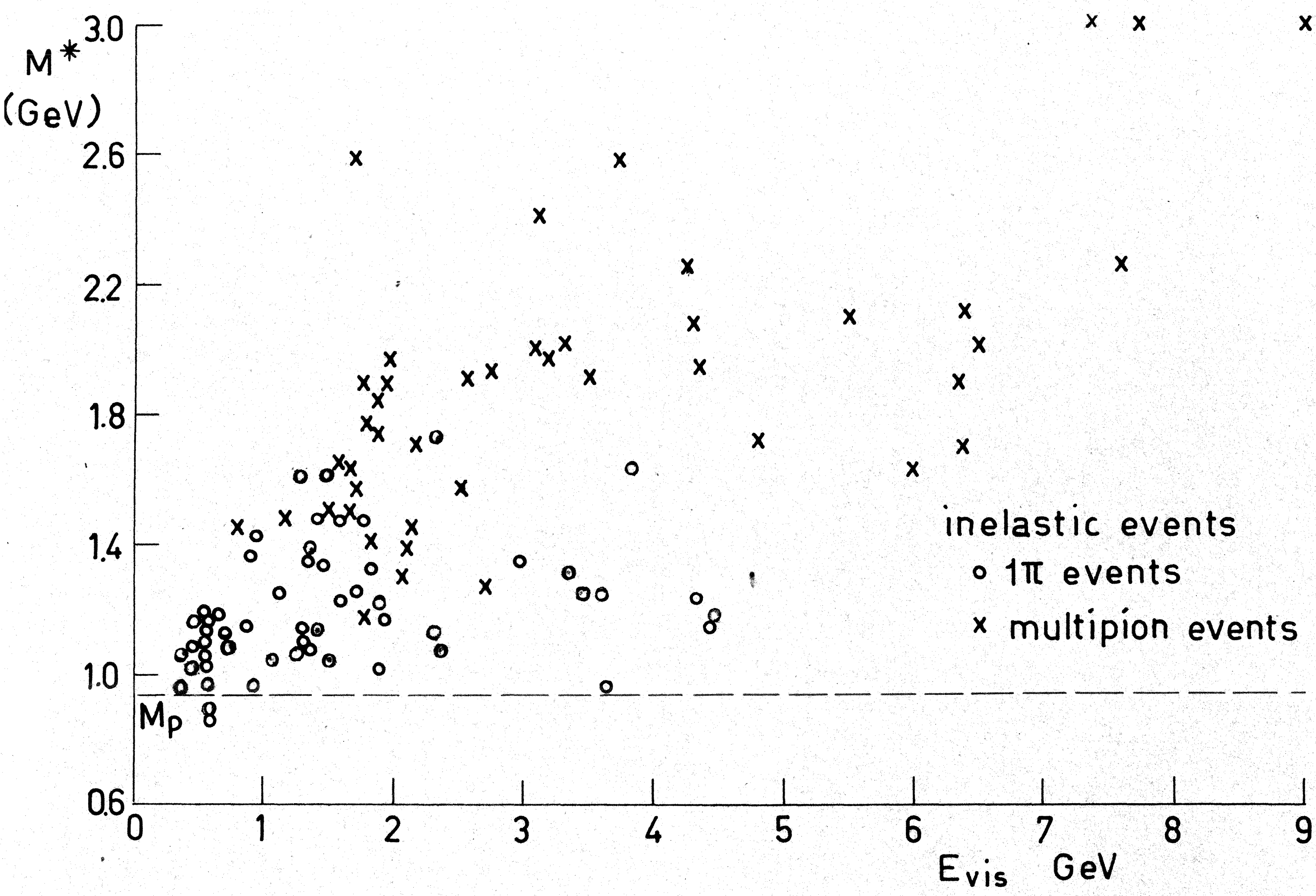
M*
(GeV)
3.0
2.6
2.2
1.8
1.4
1.0
0.6
Mp
0 1 2 3 4 5 6 7 8 9
Evis GeV
inelastic events
o 1π events
x multipion events

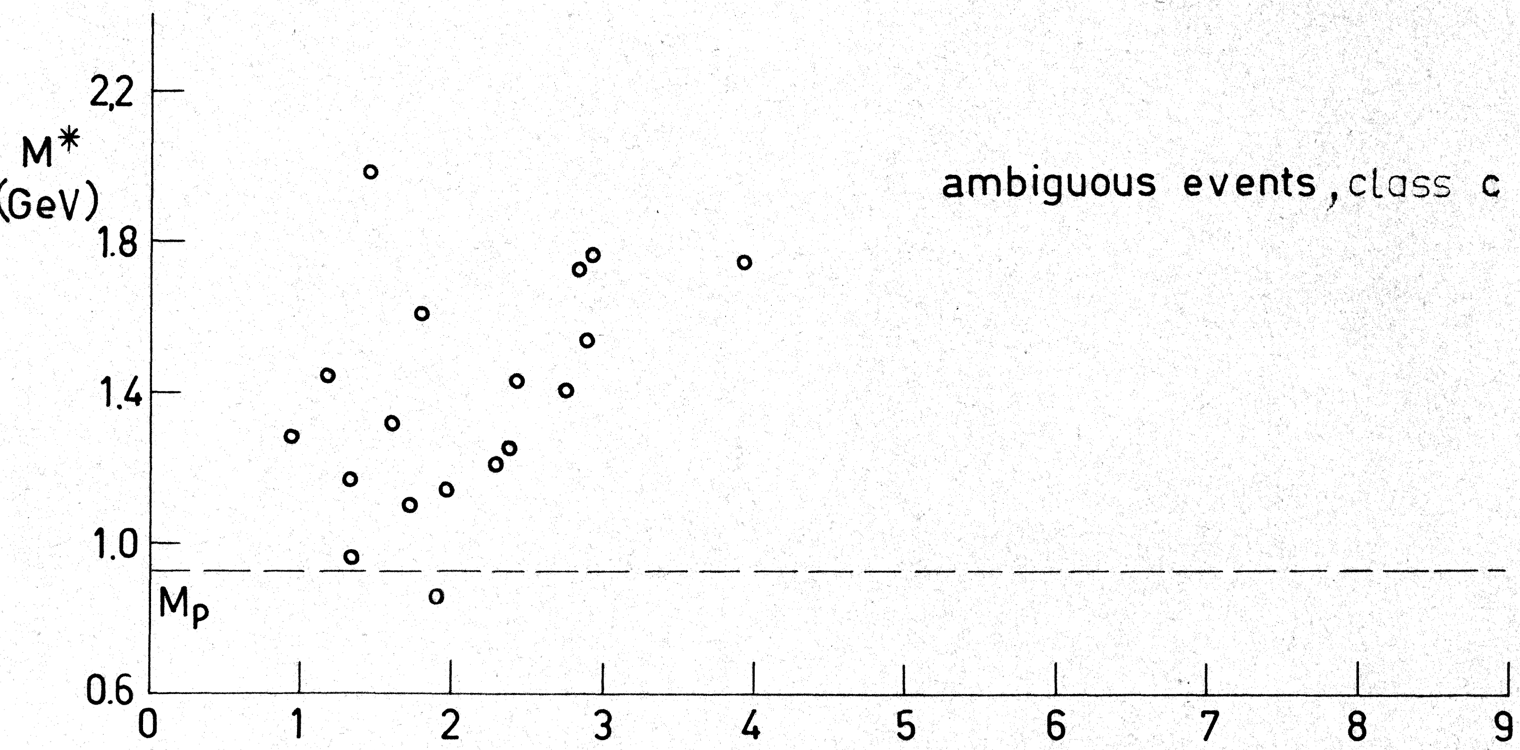
M*
(GeV)
2.2
1.8
1.4
1.0
0.6
Mp
0 1 2 3 4 5 6 7 8 9
ambiguous events, class c

Fig. 9

Fig. 10a

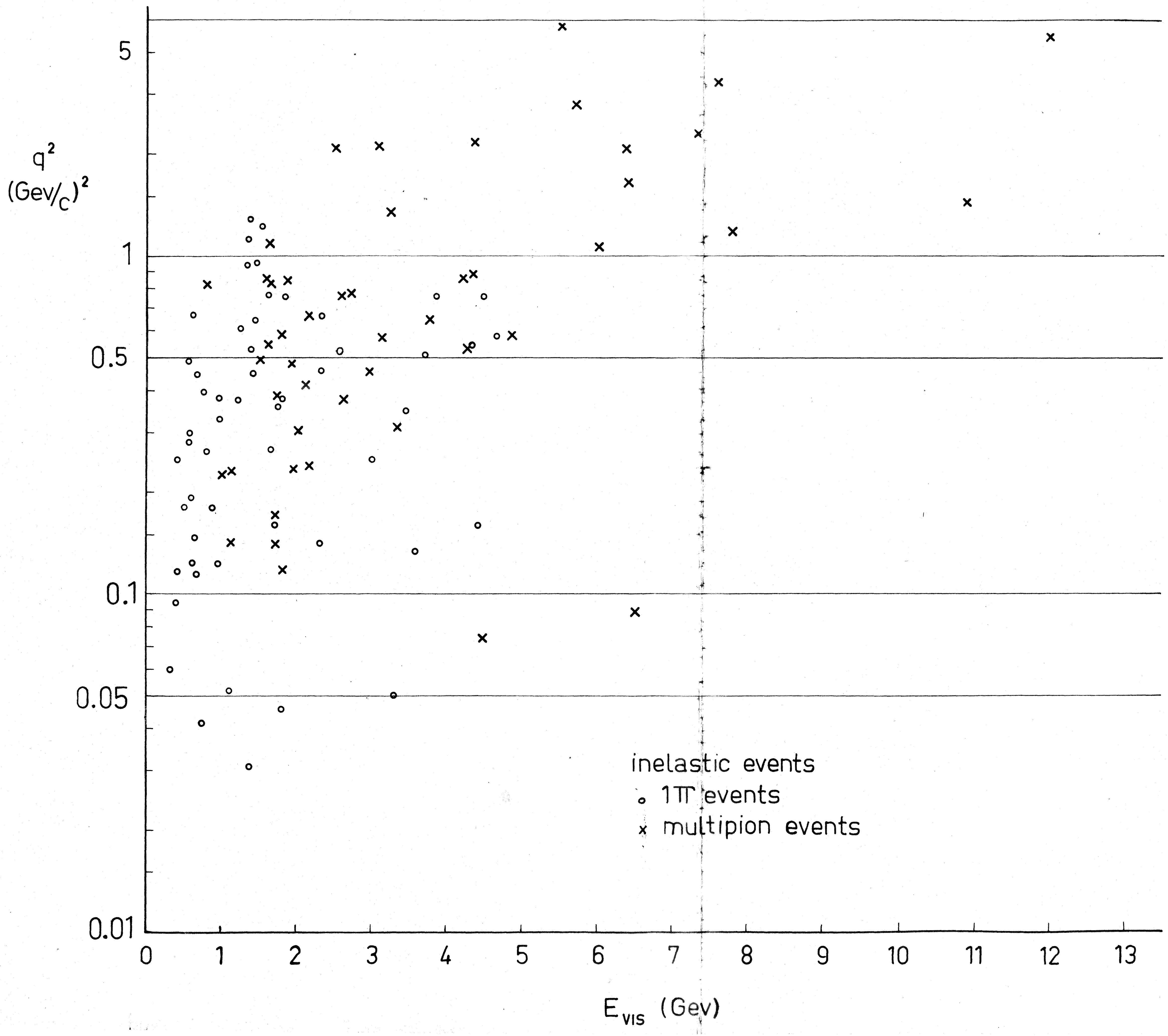

q²
(Gev/c)²
5
1
0.5
0.1
0.05
0.01
0 1 2 3 4 5 6 7 8 9 10 11 12 13
E VIS (Gev)
inelastic events
1π events
multipion events

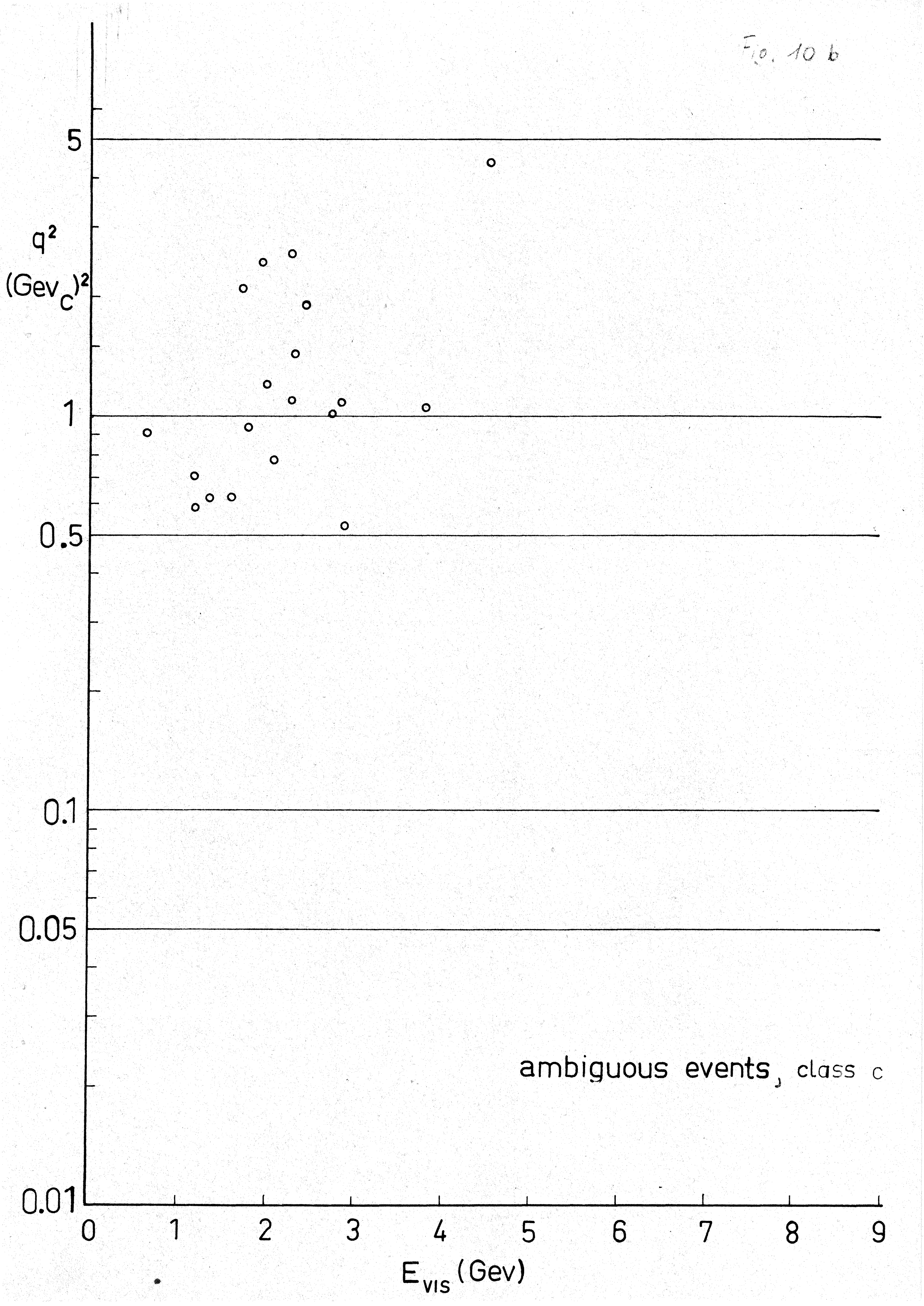

Fig. 10 b
5
1
0.5
0.1
0.05
0.01
q²
(Gev/c)²
0
1
2
3
4
5
6
7
8
9
E vis (Gev)
ambiguous events, class c

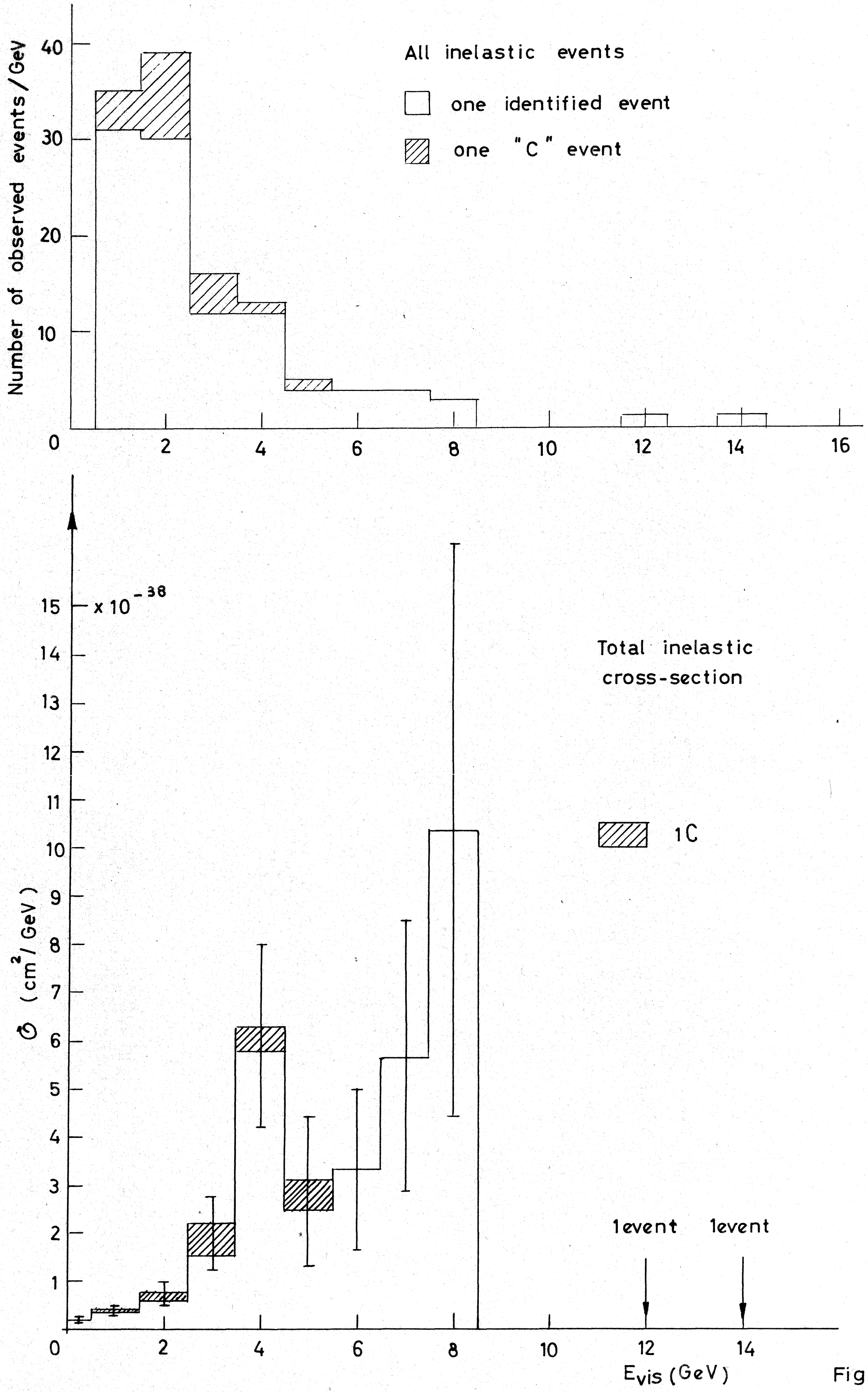

Number of observed events/GeV
All inelastic events
one identified event
one "C" event
0
10
20
30
40
2
4
6
8
10
12
14
16
σ (cm²/GeV)
x 10⁻³⁸
Total inelastic cross-section
1C
1event
1event
E_vis (GeV)

Fig.11

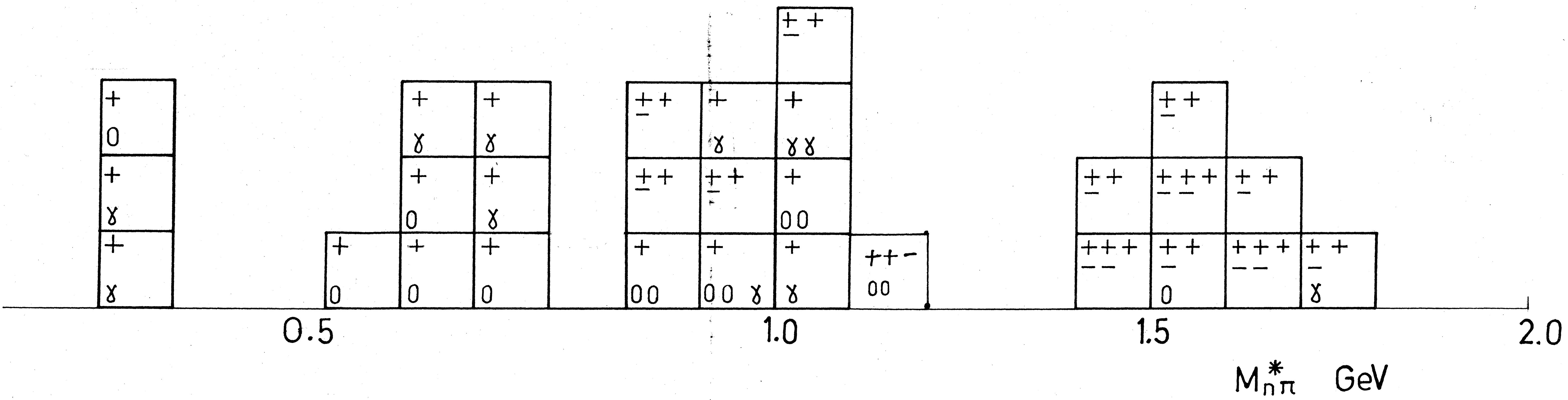

Fig 12